

Stable non-covalent functionalisation of multi-walled carbon nanotubes by pyrene–polyethylene glycol through π – π stacking†

Jie Liu,^{*a} Olivier Bibari,^a Pascal Mailley,^b Jean Dijon,^c Emmanuelle Rouvière,^c Fabien Sauter-Starace,^a Patrice Caillat,^a Françoise Vinet^a and Gilles Marchand^a

Received (in Montpellier, France) 31st July 2008, Accepted 20th November 2008

First published as an Advance Article on the web 15th December 2008

DOI: 10.1039/b813085j

Carbon nanotubes (CNTs) are good candidates to construct nanostructured, implantable micro-electrodes since they are conductive materials and may increase the overall electrode surface area, and thus the signal/noise ratio. However, the adsorption of biomolecules on CNTs is well-known to lead to a surface passivation. In this context, a surface modification appears essential to overcome these limitations. In this paper, the non-covalent functionalisation of multi-walled carbon nanotubes (MWNTs) by pyrene–PEG molecules through π – π stacking is presented. We describe in the first part the functionalisation of MWNT powders in aqueous solution for which we obtained a stable dispersion of functionalised MWNTs. The stability of the non-covalently functionalised MWNT dispersion during 7 cycles of dialysis in H₂O was studied by UV spectroscopy. The density of pyrene–PEG on the MWNT surface stabilised at about 4×10^{11} molecules mm^{−2} after 4 cycles of dialysis (all the free pyrene–PEG molecules were removed by dialysis). Next, this non-covalent functionalisation of MWNT arrays on a substrate was examined. After the functionalisation, the increase of the MWNT wettability led to a 50-fold increase of the capacitance of the MWNT nanostructured electrode. Finally, we chose streptavidin, a well-known adhesive protein, as an example to test the efficiency of functionalised MWNTs towards preventing non-specific adsorption. The result shows that the presence of pyrene–PEG on the MWNT surface is indeed efficient.

Introduction

In recent years, researchers have developed systems to interface living cells, such as neurons, with electronics to create a brain–computer interface (BCI) system using micro-electrodes and so to record action potentials.^{1,2} The use of electrodes with a nanostructured surface can be a way to: (i) make small diameter electrodes with large active surface areas, (ii) increase the signal intensity, (iii) increase the signal to noise ratio and consequently improve the electrode sensitivity. In this way, carbon nanotube (CNT) arrays can be good candidates to make nanostructured, electrically conductive and implantable micro-electrodes. Indeed, CNTs allow an increase in the overall surface area leading to a higher signal and tend to reduce the electrode output impedance and increase its capacitance. Consequently, the signal to noise ratio is increased by limiting the thermal noise proportional to the interfacial impedance.³ However, the design of implants with stable electrical properties in long-term applications is still a challenge since the

non-specific adsorption of some proteins can generate the formation of fibroblasts around the electrodes, which degrade their electrical performance over time. A functionalisation of the CNTs may be an efficient way to prevent the adsorption of these bio-molecules.

Polyethylene glycol (PEG) is a biocompatible polymer which has been widely used in the field of biology to create hydrophilic surfaces and to prevent the non-specific adsorption of bio-molecules on the surface. The functionalisation of CNT-covered electrodes by PEG chains may be an efficient way to prevent the non-specific adsorption of some bio-molecules on the surface. Many works have been reported on the functionalisation of single-walled carbon nanotubes (SWNTs) by PEG chains. For example, after oxidation of SWNTs, the generated carboxylic groups have been modified in acyl chloride groups which can react with hydroxyl-terminated PEG to give PEG-chain covalently-functionalised SWNT bundles.^{4,5} PEGylated individual SWNTs have also been obtained through doping by lithium to undo the bundles before reacting with PEG chains.⁶ However, the covalent functionalisation can introduce defects on the sidewall of CNTs, which will reduce their electrical conductivity.⁷ To overcome this problem, several works have been described on the non-covalent functionalisation of CNTs by PEG chains: (i) adsorption of PEG chains onto SWNTs assisted by Triton X-100 or Triton X-405;⁸ (ii) adsorption of PEG–phospholipids on the SWNTs through hydrophobic interaction;⁹ (iii) functionalisation of SWNTs by

^a CEA-LETI-DTBS Minatec, 17 rue des Martyres, 38054 Grenoble, France. E-mail: jie.liu@cea.fr; Tel: +33 (0)4 38 78 21 46

^b CEA-DSM-DRFMC, 17 rue des Martyres, 38054 Grenoble, France

^c CEA-LITEN-LCH, 17 rue des Martyres, 38054 Grenoble, France

† Electronic supplementary information (ESI) available: NMR and MS spectrum of pyrene-PEG; calibration curve of MWNTs; TGA curve of MWNT-1 after 7 cycles of dialysis; XPS C 1s results of MWNTs/Si functionalised with only MeO-PEG-NH₂; XPS results of MWNTs/Si and *f*-MWNTs/Si before and after the adsorption of streptavidin. Angle contact measurements. See DOI: 10.1039/b813085j

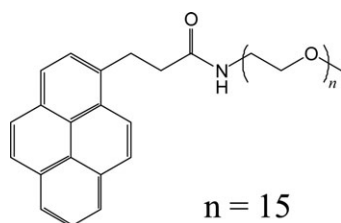
Fluorescein-PEG molecules.¹⁰ These authors have shown good resistance to the non-specific binding of proteins, stability at high temperature (80 °C) and strong ionic strengths.

In this paper, we present in the first part the non-covalent functionalisation of multi-walled carbon nanotube (MWNT) powders in aqueous solution by pyrene-PEG through π - π stacking. Analysis of the results shows an effective functionalisation and a strong interaction between the CNT surface and the pyrene-PEG molecules. This non-covalent functionalisation appears stable under extreme pH conditions and in strong ionic strength solutions. Secondly, this functionalisation method was applied to functionalise MWNT arrays on a substrate through a simple incubation in pyrene-PEG solution; we characterised the MWNT arrays by XPS, wettability and electrochemical methods. In the final part, the efficiency of functionalised MWNT arrays in preventing the non-specific adsorption of streptavidin on the MWNT array surface was shown.

Experimental

Materials and reagents. Purified MWNT powder was purchased from Nanocyl S.A. (NC3100). α -Methoxy- β -amino poly(ethylene glycol) (750 Dalton, polydispersity = 1.1) was purchased from Iris Biotech GmbH. Phosphate buffer solution (PBS) (10 \times , pH 7.4) was purchased from Euromedex and diluted (1 \times) with water for biological tests. Quantum dots covered by streptavidin (Qdots-streptavidin), with an emission at 605 nm, were purchased from Invitrogen Sarl (Ref. Q10101MP). All other reagents were purchased from Sigma-Aldrich and used without further purification.

Synthesis of pyrene-PEG 1. 5 ml of α -methoxy- β -amino poly(ethylene glycol) (~0.7 mmol) solution in dimethylformamide (DMF) was slowly added to 5 ml of a stirred solution of 1-pyrenebutanoic acid succinimidyl ester (1 mmol) in DMF under inert atmosphere. After 24 h at room temperature, DMF was removed under vacuum and the brown residue was purified by chromatography on alumina (CH₂Cl₂-MeOH = 98 : 2). A white oil was obtained with a yield of 46%. ¹H NMR (200 MHz, [D₆] DMSO): δ = 2.04 (m, 2H), 2.25 (t, J = 7 Hz, 2H), 3.22 (s, 3H), 3.23–3.6 (m, 66H), 7.9–8.42 (m, 9H). Multiple mass spectrometry peaks were observed due to the polydispersity of PEG. ESI-MS m/z : 808.5; 852.5; 896.5; 940.5; 984.5 (M + Na with n = 15); 1028.5; 1072.5; 1116.6; 1160.5; 1204.6; 1248.5; 1292.6; 1336.7. The structural formula of the pyrene-PEG 1 is shown in Scheme 1.



Scheme 1 Structural formula of the pyrene-PEG 1.



Fig. 1 Dispersions of MWNT-1 in different solutions after settling for 1 week. A: MWNT-1 after dialysis; B: MWNT-1 in 1 M NaOH; C: MWNT-1 in 0.1 M NaOH; D: MWNT-1 in 0.5 M NaCl; E: MWNT-1 in 0.1 M HCl; F: MWNT-1 in 1 M HCl; G: MWNT-1 in physiologic buffer (PBS 10 \times); H: oxidised MWNT-1 in 0.1 M HCl; I: oxidised MWNTs in 0.1 M HCl.

Functionalisation of MWNT powders. 7 mg of MWNTs were added to 10 ml of pyrene-PEG solution (6 mM) in H₂O. The mixture was treated using an ultrasonic bath (100 W) for 3 h at room temperature. After sonication, the MWNT suspension was centrifuged at 24 000 g for 3 h, and the black supernatant was collected. Next, 1 ml of the MWNT suspension was diluted by H₂O to 30 ml and submitted to dialysis in H₂O to remove the free pyrene-PEG molecules in the suspension. The dialysis H₂O was changed every day until elimination of molecules 1 in the dialysis water (probed by UV spectroscopy). After the dialysis, the MWNT suspension was centrifuged at 10 000 g for 2 h. A transparent stable suspension of MWNTs was obtained (Fig. 1, sample A). The functionalised MWNTs are named MWNT-1.

Determination of pyrene-PEG density on the MWNT surface in an aqueous dispersion containing MWNT-1 and free 1 molecules. The density of pyrene-PEG 1 on the surface of MWNT-1 was determined by UV-Vis absorption spectroscopy.

(i) First, the calibration curve (absorbance = f (concentration)) of 1 was established at 342 nm.

In order to realise the MWNT calibration curve, 30 mg of MWNTs were added to 30 ml of a sodium dodecyl sulfate (SDS) aqueous solution (1 wt%). The mixture was treated using an ultrasonic bath (100 W) for 3 h. Then the suspension was centrifuged at 24 000 g for 3 h to remove the aggregated MWNTs and the supernatant was collected. The MWNT concentration in this suspension was measured using the following protocol: 100 ml of acetone were added to 10 ml of the obtained MWNT-SDS suspension to precipitate the MWNTs which were then collected by centrifugation to remove SDS. The rinse with acetone was repeated three times and MWNTs were collected on a PTFE filter (0.2 μ m) in the final step. The collected MWNTs were dried in vacuum at 80 °C for 24 h, and weighed (1.6 mg). So the concentration of MWNTs in the suspension (stabilised by SDS) was determined to be about 160 μ g ml⁻¹.

The MWNT calibration curve was plotted by diluting 10 to 500 μ l of the obtained MWNT-SDS suspension with 4 ml SDS aqueous solution (1 wt%). The UV-Vis spectra of the diluted suspensions were recorded using a SDS solution (1 wt%) as reference, and the absorbance of MWNTs at 254 nm was used to plot the calibration curve (Fig. S2, ESI[†]).

(ii) Secondly, the density of 1 on the MWNT-1 surface in a suspension containing MWNT-1 and free 1 molecules was determined by UV-Vis spectroscopy. In the following

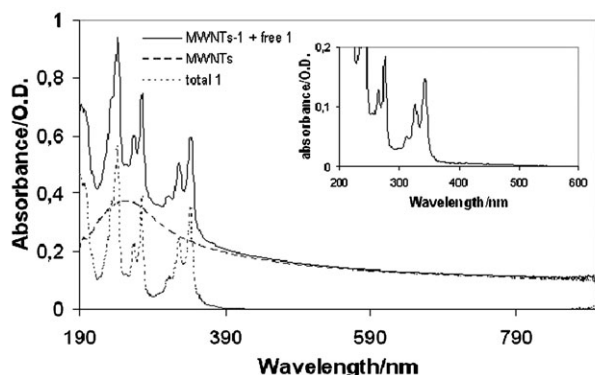


Fig. 2 Determination of density of molecules **1** on the surface of MWNT-**1**. Solid line: absorption spectrum of MWNT-**1** + free **1**. Dashed line: absorption spectrum of MWNTs stabilised by SDS. Dotted line: the difference between the two spectra represents the absorption of all the **1** in functionalised MWNTs. Inset: absorption spectrum of filtrate of functionalised MWNTs by molecules **1**.

protocol, all solutions were diluted before UV-Vis spectroscopy measurements to ensure that the absorbance of MWNT-**1** and **1** is in the linear zone of their calibration curve.

To prepare a suspension containing MWNT-**1** and free **1** molecules, 1 mg of MWNTs was dispersed in 2 ml of an aqueous solution of **1** (6 mM) by an ultrasonic bath (3 h), followed by centrifugation at 24 000 *g* for 3 h to eliminate the aggregated, non-functionalised MWNTs. 1 ml of the supernatant was collected and diluted to 30 ml by H₂O. The diluted MWNT-**1** suspension was dialysed in 2 l of H₂O for 24 h and then submitted to centrifugation at 10 000 *g* for 2 h. Fig. 2 (solid line) shows the spectrum of this suspension containing MWNT-**1** and free **1**.

To obtain the total concentration of **1** (**1** on the surface of MWNT-**1** + free **1**) in the suspension, the contribution of MWNTs in the spectrum of Fig. 2 (solid line) was subtracted by a spectrum of MWNTs stabilised by SDS with an intensity of absorption near to that of MWNT-**1** at 600 nm, at which wavelength **1** does not absorb. The spectrum of MWNTs-SDS was multiplied by a constant to make the two spectra overlap between 500 nm and 800 nm (Fig. 2, dashed line). After removal of the MWNT contribution to the spectrum of Fig. 2 (solid line), we obtain a spectrum typical of pyrene-PEG **1** (Fig. 2, dotted line); it represents the absorption of all pyrene-PEG molecules in the suspension, and is attributed to **1** on the surface of MWNT-**1** and free **1**. From this spectrum (Fig. 2, dotted line), the total concentration of **1** ([**1** total]) in the suspension using the calibration curve of **1** was calculated.

To determine the concentration of free **1**, the suspension containing MWNT-**1** and free **1** was filtered to remove MWNT-**1**. In order to avoid the evaporation of solvent during the filtration, a PES filter (pore size: 0.1 μ m) on syringe was used. The filtrate spectrum is shown in the inset of Fig. 2. We suggest that the concentration of **1** in the filtrate corresponds to that of free **1** in the suspension ([Free **1**]). The concentration of **1** on the MWNT-**1** surface ([**1** on MWNT-**1**]) was calculated from the difference between the total concentration of **1** in the suspension and that of the free **1** in the filtrate: [**1** on MWNT-**1**] = [**1** total] – [Free **1**].

The concentration of MWNT-**1** [MWNT-**1**] in the suspension was calculated from the spectrum of Fig. 2 (dashed line) using the calibration curve of MWNTs.

The surface area of the MWNTs is calculated from the formula given by Peigney *et al.*¹¹ Our MWNTs have an average diameter of ~ 8 nm, with an average number of walls of 6, based on TEM. The calculated outside surface area is 270 m² per gram.

With the given concentration of MWNTs, the concentration of **1** on the surface of MWNT-**1**, and the MWNT surface area, we can then calculate the density of molecule **1** on the MWNT surface:

density (molecule mm⁻²)

$$= \frac{6.02 \times 10^{23} (\text{molecules mol}^{-1}) \times [\text{1 on MWNT}] (\text{mol l}^{-1})}{2.7 \times 10^8 (\text{mm}^2 \text{ g}^{-1}) \times [\text{MWNT} - \text{1}] (\text{g l}^{-1})}$$

A TGA analysis was carried out to verify the accuracy of the calculated density of **1** on MWNT-**1** by absorption spectroscopy: a suspension of MWNT-**1** after removal of all free **1** molecules was filtered through a PES membrane (pore size: 0.2 μ m). The recovered MWNT-**1** was dried in vacuum at 50 °C for 3 days and submitted to TGA analysis. The TGA analysis was performed in inert atmosphere, temperature was increased from room temperature to 550 °C at 10 °C per minute.

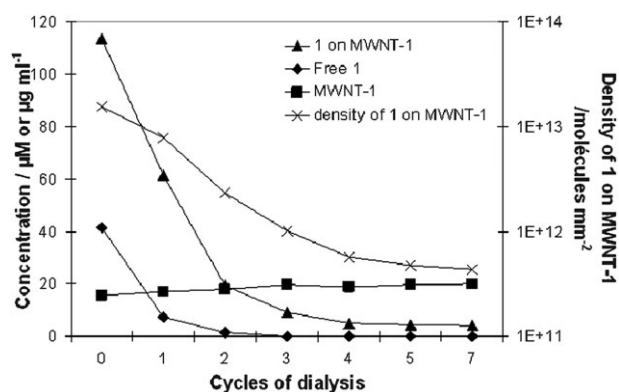
Study of the variation of density of **1 on MWNT-**1** during dialysis.** The variation of the concentration of MWNT-**1** and of the density of **1** on the surface of MWNT-**1** in a functionalised MWNTs suspension was followed during dialysis of 7 cycles.

In a typical experiment, 2 mg of MWNTs were dispersed in 4 ml of an aqueous solution of **1** (6 mM) by an ultrasonic bath (3 h), followed by centrifugation at 24 000 *g* for 3 h to eliminate the aggregated, non-functionalised MWNTs. 2 ml of the supernatant were collected and diluted to 60 ml by H₂O. 7 ml of this diluted MWNT-**1** suspension, containing free **1**, were preserved and submitted to centrifugation at 10 000 *g* for 2 h. The concentration of MWNT-**1** and the density of **1** on MWNT-**1** in this suspension were determined by the method described above (Table 1). The rest of the diluted suspension (53 ml) was submitted to dialysis (membrane CELLU-SET T1 3500 Da) in H₂O (1 l). The dialysis water was changed every 24 h for 7 days, and 7 ml of the suspension were preserved after every cycle of dialysis. The preserved suspension was submitted to centrifugation at 10 000 *g* for 2 h before determination of concentrations and density of **1**. The dialysis water was also analysed by UV-Vis spectroscopy after every dialysis cycle. The concentration of MWNT-**1** and of **1**, and the density of molecule **1** on the surface of MWNT-**1** for 7 cycles of dialysis are calculated and listed in Table 1 and Fig. 3.

MWNT synthesis on silicon substrate. Two kinds of samples were considered in this study, MWNT arrays (MWNTs/Si) and MWNT array-covered electrodes. In both cases, MWNTs were grown on a silicon substrate coated with a layer of silicon oxide (SiO₂, 1 μ m thick) and titanium nitride (TiN, 300 nm

Table 1 Variation of concentration of MWNT-1, **1** during the dialysis, and the density of pyrene-PEG on the surface of MWNTs

| | MWNT-1/ $\mu\text{g ml}^{-1}$ | 1 on MWNT-1/ μM | Free 1 / μM | 1 in dialysis $\text{H}_2\text{O}/\mu\text{M}$ | Density of 1 on MWNT-1/molecules mm^{-2} | % of coverage of MWNTs |
|--------------------------|-------------------------------|-----------------------------------|-------------------------------|---|--|------------------------|
| Diluted, before dialysis | 15.7 | 113.5 | 41.5 | NA | 1.6×10^{13} | 720 |
| 1 Dialysis | 17.0 | 61.6 | 7.4 | 8.26 | 7.8×10^{12} | 361 |
| 2 Dialysis | 18.0 | 19.4 | 1.6 | 2.00 | 2.3×10^{12} | 107 |
| 3 Dialysis | 19.8 | 9.6 | 0 | 0.86 | 1.0×10^{12} | 47 |
| 4 Dialysis | 18.7 | 5.0 | 0 | 0 | 5.8×10^{11} | 26 |
| 5 Dialysis | 19.6 | 4.3 | 0 | 0 | 4.7×10^{11} | 22 |
| 7 Dialysis | 20.0 | 4.1 | 0 | 0 | 4.4×10^{11} | 20 |

**Fig. 3** Variation of concentrations of MWNT-1, free **1**, **1** on the surface of MWNTs and the density of **1** on MWNT-1 during 7 cycles of dialysis in H_2O .

thick). The SiO_2 and TiN layers were deposited by chemical vapour deposition (CVD). In the case of MWNT electrode, the substrate was patterned by UV photolithography and dry etching (SF_6 plasma) techniques to define electrodes ($\varnothing = 150 \mu\text{m}$), conductive lines and contact pads of the matrix. A silicon nitride (Si_3N_4) layer of 500 nm was deposited and then etched by a plasma (CF_4/O_2) to open windows for the TiN electrodes and pads. Next, a 5 nm nickel layer was deposited by CVD on the full TiN layer for MWNTs/Si and specifically on TiN electrodes by the lift-off technique for MWNT electrode. Finally, growth of the MWNTs on the electrode was realised by CVD at 600 °C in an atmosphere composed of acetylene and hydrogen at low pressure for 15 min.

Functionalisation of MWNT arrays. To functionalise the MWNT arrays, the sample with MWNT arrays was incubated in 10 ml of pyrene-PEG solution (2 mM) in H_2O for 24 h. Next, the sample surface was rinsed thoroughly with distilled water ($3 \times 20 \text{ ml}$) to remove the free pyrene-PEG molecules and dried under vacuum at room temperature. The final samples are named *f*-MWNTs/Si.

Non-specific adsorption of streptavidin. MWNTs/Si or *f*-MWNTs/Si were incubated in a Qdots-streptavidin or streptavidin solution (15 nM) in PBS (phosphate buffer saline, $1\times$, pH = 7.4) for 18 h. Next, the samples were rinsed in PBS ($1\times$) solution for 3 h to remove the free streptavidin and washed one more time with PBS, three times with de-ionised water and then dried.

Characterisation. The UV-Vis spectra were determined on a CARY 300 scan UV-Visible spectrophotometer. The XPS analyses were performed on an S-probe instrument using Al K α (1486 eV) monochromatic electron source. The deconvolutions of the C 1s peaks were performed using the XPS Peak software. The contact angle was measured with a GBX Digidrop instrument. The electrochemistry was realised on a Princeton Applied Research 283 potentiostat. The centrifugation of CNT suspensions was performed using a Prolabo SR4000 instrument.

Results and discussion

The non-covalent functionalisation of the CNTs by substituted pyrene through π - π stacking has been widely described in the literature.¹²⁻¹⁵ This functionalisation consists in the specific recognition between the π - π skeleton of the CNTs and a pyrene moiety due to the delocalised π -electrons. An aromatic interaction is a non-covalent interaction between organic compounds containing aromatic moieties. π - π interactions are caused by intermolecular overlapping of p-orbitals in π -conjugated systems, so they become stronger as the number of π -electrons increases.

In order to characterise the functionalisation, especially to determine the density of **1** on the MWNT-1 surface, the functionalisation was firstly developed on MWNT powders and next transferred to the well-established protocol on the MWNTs arrays.

Functionalisation and characterisation of MWNT powders

The functionalisation was performed by sonication of a mixture of MWNTs and **1** in aqueous solution. The non-dispersed MWNTs after sonication were removed by centrifugation, and a black, stable functionalised MWNT suspension was obtained. This suspension is composed of functionalised MWNTs (MWNT-1) and free **1** molecules. After dilution and dialysis to remove the free **1** molecule, a stable MWNT-1 suspension was obtained (Fig. 1, sample A). There is no more **1** detectable in the dialysis H_2O after 4 cycles of dialysis (Table 1) and therefore, in the MWNT-1 suspension. This result suggests that the MWNTs, initially insoluble in water, have been functionalised by **1** which allows their dispersion.

It has been reported in the literature that CNTs can be functionalised by trimethyl-(2-oxo-2-pyren-1-yl-ethyl)-ammonium bromide, a pyrene-carrying ammonium ion (pyrene-ammonium), through π - π stacking, the molecules are in dynamic equilibrium between the bulk phase and the sidewalls of the CNTs.

Dialysis of the functionalised CNTs by pyrene-ammonium caused a gradual precipitation of the CNTs.¹⁶ Instead of ammonium, here we used a PEG chain to substitute the pyrene moiety. The MWNT-1 remains stable in suspension even after all the free **1** molecules have been removed. Dai *et al.*¹⁰ have also reported the functionalisation of SWNTs by Fluor-PEG, and the functionalised SWNT suspension remained stable after removal of free Fluor-PEG molecules. This result shows that the PEG chain may help the functionalisation of **1** on the surface of CNTs.

The stability of the functionalisation of MWNTs by pyrene-PEG **1** is studied by following the change of MWNT-1 and **1** concentrations, and the density of **1** on the MWNT-1 during each cycle of dialysis. The concentration of MWNT-1, the total concentration of **1**, free **1** and **1** in the dialysis H₂O was measured by UV-Vis spectroscopy. The densities of **1** were calculated by the method described in the experimental section. These data are listed in Table 1 and Fig. 3.

We observed that dialysis is efficient in removing the free **1** molecules in the MWNT-1 suspension. Indeed, the concentration of free **1** ([Free **1**]) decreases rapidly to 0 after 3 cycles of dialysis (Table 1). The concentration of **1** in dialysis H₂O is a little higher than that of free **1**, and decreased to 0 after 4 cycles of dialysis. So, 4 cycles are enough to remove the free **1** molecules in the suspension.

The concentration of **1** on the surface of MWNT-1 ([**1** on MWNT-1]) is always far greater than [free **1**] in the suspension (Table 1). This means that the interaction between **1** and the surface of MWNTs is strong and pyrene-PEG molecules absorbed on the MWNT surface rather than in the solution. The concentration of **1** on MWNT-1 ([**1** on MWNT-1]) decreased rapidly over the first 3 cycles of dialysis, and stabilised at about 4 μM after 7 cycles (Fig. 3). On the contrary, the concentration of MWNT-1 increased slowly over the first 3 cycles of dialysis. In fact, there is a diminution of the total volume of MWNT-1 suspension after the 7 cycles of dialysis: only ~ 2 ml of MWNT-1 suspension rested instead of 11 ml after the preservation during the dialysis. This can explain the increase of MWNT-1 concentrations. As the concentrations of MWNT-1, free **1** and **1** on MWNT-1 were measured independently after each dialysis, this diminution of volume will not change the calculated density of **1** on MWNT-1.

The density of **1** on the MWNT-1 surface calculated from concentrations of MWNT-1 and concentrations of **1** on MWNT-1 is 1.6×10^{13} molecules mm^{-2} in the diluted and non-dialyzed suspension. This density decreases rapidly during the first 3 cycles of dialysis and more slowly during the last 4. It stabilised at about 4×10^{11} molecules mm^{-2} (Fig. 3). The density of **1** on MWNT-1 was also calculated by TGA analysis after removal of all free **1** molecules to compare with the result obtained by UV-Vis absorption spectroscopy. We observed a weight loss of 22 wt% in TGA analysis for collected and dried MWNT-1 sample (Fig. S3, ESI†). The weight loss began at about 200 °C and finished at about 400 °C. This weight loss is attributed to the mass of **1** in the MWNT-1. The density of **1** in MWNT-1 calculated from this weight loss using the MWNTs surface area of $270 \text{ m}^2 \text{ g}^{-1}$ and average **1** molecules mass of 961.5 g mol^{-1} (data obtained from mass spectroscopy) is

6.5×10^{11} molecules mm^{-2} . This value is generally incoherent with the result obtained by absorption spectroscopy, in which an error may be introduced during the subtraction of the MWNT-1 spectrum by a MWNTs-SDS spectrum, because the background absorption of MWNTs stabilised by SDS and by **1** may not be the same.

The proportion of MWNT-1 surface covered by a pyrene moiety in percentage is calculated from the density of **1** on the MWNT-1 surface. First the surface area of a pyrene ring is simulated from ChemBio3D to be 0.46 nm^2 (using MM2 minimised energy). Then, the proportion of covered surface in percentage (PC) is calculated through the following formula: $\text{PC} = 0.46 (\text{nm}^2 \text{ molecule}^{-1}) \times \text{density of } 1 (\text{molecule mm}^{-2}) \times 100$. The calculated PC is listed in Table 1. The PC of diluted and non-dialyzed suspension of MWNT-1 is 720% (Table 1); this suggests that there is more than one layer of **1** on the surface of MWNT-1 in this sample. We think that at a high concentration of pyrene-PEG, the interaction between the PEG chains can confine the pyrene-PEG on the surface of MWNTs, which formed a multi-layer coverage of the MWNT-1. However, this interaction between the PEG chains is relatively weak since the multi-layer can be removed by dialysis. After 7 cycles of dialysis (removal of the entire free **1**), the PC stabilised at about 20%.

The stability of the functionalisation is also studied under extreme pH conditions. In a typical experiment, 67 μl of concentrated MWNT-1 was diluted in 2 ml of the desired solution and the suspension was left to settle for 1 week. Fig. 1, samples B–F show the MWNT-1 in 1 M NaOH, 0.1 M NaOH, 0.5 M NaCl, 0.1 M HCl, 1 M HCl. These suspensions are stable after settling for 1 week; we observed only a small amount of precipitate at the bottom in 1 M NaOH (Fig. 1, sample B) and 1 M HCl (Fig. 1, sample F) suspensions, and no precipitate in the other solutions. The MWNT-1 is also stable in PBS even at a high concentration, $10\times$ (Fig. 1, sample G). These results show that the functionalised MWNTs are stable in strong basic and acidic conditions, and also in high ionic strengths.

Fig. 1, sample H, shows the suspension of oxidised MWNTs functionalised by **1** in 0.1 M HCl; it is also stable, no obvious precipitate being observed after settling for 1 week. On the contrary, the oxidised MWNTs precipitate very fast in 0.1 M HCl without pyrene-PEG (Fig. 1, sample I). HCl treatment is usually necessary after oxidation of CNTs to transfer carboxylate to carboxylic groups for further functionalisation of CNTs. But the CNTs with carboxylic groups are barely soluble in aqueous solutions, which make the reactions inhomogeneous. The functionalisation of oxidised MWNTs with pyrene-PEG makes it possible to have a homogeneous reaction between CNTs and biological molecules, such as DNAs and proteins, in aqueous solution.

Functionalisation and characterisation of MWNT arrays

The above results show that MWNTs can be functionalised with pyrene-PEG molecules **1** by π - π stacking and the interaction **1**/MWNTs is relatively strong. This makes it possible to non-covalently functionalise the MWNT arrays on silicon by this method. MWNTs/Si ($1 \times 1 \text{ cm}$) was incubated in an

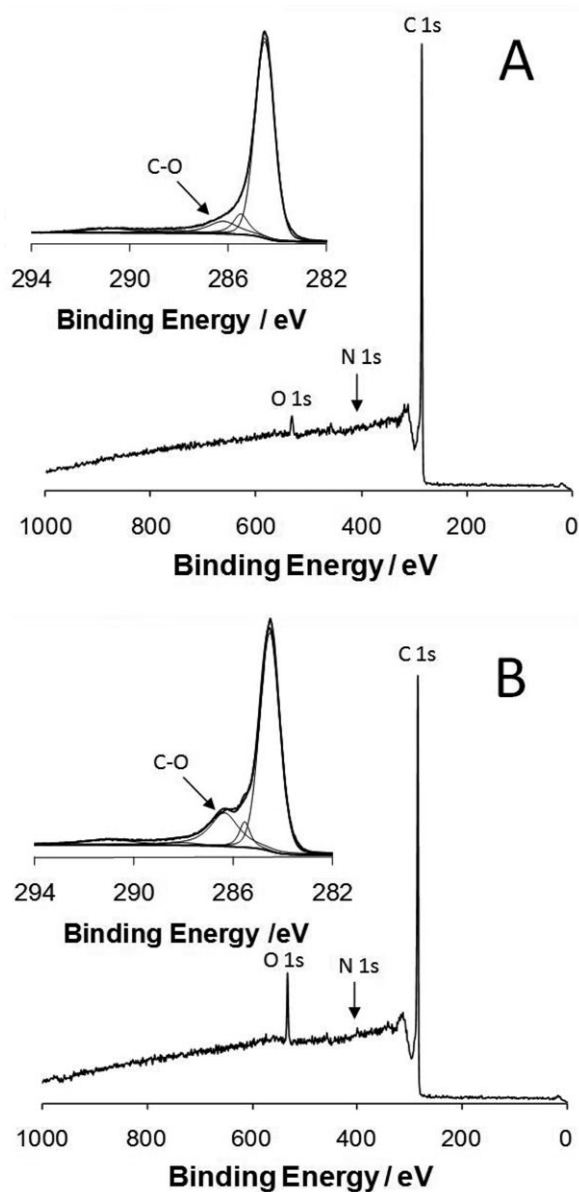


Fig. 4 XPS survey scans of MWNTs/Si (A) and *f*-MWNTs/Si (B). Atomic percentages of elements in MWNTs/Si: C, 96.5%; O, 2.7%; N, 0.8%. In *f*-MWNTs/Si: C, 91.1%; O, 7.9%; N, 1.0%. Inset: deconvolution of XPS C 1s peak.

aqueous solution containing **1** for 24 h and thoroughly rinsed with water to remove the free pyrene-PEG molecules. These samples were first characterised by XPS (Fig. 4). In the non-functionalised MWNTs/Si, we observed 2.7% of oxygen atoms coming from the defects on the MWNTs and 0.8% N atoms due to the TiN layer (which is confirmed by the deconvolution of the N 1s peak, data not shown here). The low percentage of nitrogen atoms shows that the TiN surface was almost totally covered by MWNTs. After the functionalisation, an increase of the O%, from 2.7% to 7.9%, due to the presence of pyrene-PEG molecules in the *f*-MWNTs/Si sample, is observed. The deconvolution of the XPS C 1s spectra of MWNTs/Si and *f*-MWNTs/Si was performed with a Shirley baseline and five Voigt lines to fit the C 1s spectra

(Fig. 4, inset).¹⁷ After the functionalisation by pyrene-PEG molecules, the component which corresponds to carbons bonded to an oxygen through a single bond (C–O) is strongly increased (Fig. 4, inset). Indeed, the PEG chains contain a large number of C–O bonds, and so the increase in the C–O component indicates the presence of pyrene-PEG molecules on the *f*-MWNTs/Si surface. Note that a control experiment was carried out to check the π - π stacking by incubating MWNTs/Si in an aqueous solution of MeO-PEG-NH₂ (750 Dalton) (2 mM) for 24 h, then washed thoroughly with distilled water and characterised by XPS. In this case, no obvious modification of the XPS spectrum of MWNTs was observed (Fig. S4, ESI†). These results confirm that the pyrene-PEG molecules immobilised on the MWNTs surface through interaction between the pyrene moiety and the MWNTs.

The functionalisation of MWNTs/Si by **1** can modify the wettability of the MWNTs/Si surface. The contact angle of a distilled water drop on the MWNTs/Si surface before and after the functionalisation was measured; we obtained a contact angle of 153° on the non-functionalised MWNTs/Si whereas it becomes 28° after functionalisation (Fig. S5, ESI†). This change can be explained by the presence of the very hydrophilic PEG chains on the surface.

Finally, electrochemical measurements, cyclic voltammetry and ac-impedance spectroscopy were carried out on MWNT array-covered electrodes, which have a diameter of 150 μ m (Fig. 5A, inset), to investigate the impact of functionalisation on electrode electrical characteristics. The MWNT electrode was functionalised with the same procedure described before, and the electrochemical behaviour was measured before and after the functionalisation by **1** to specifically assess the capacitive comportment of the MWNT array. Impedance measurements were carried out at open circuit potential by applying a modulated potential (10 mV rms, frequency range 10 mHz–50 kHz) in a KCl solution (1 M). Fig. 5A displays the Nyquist plot of the impedance spectra related to **1** functionalised (*f*-MWNT) and non-functionalised MWNT arrays. These impedance spectra were fitted using the electrical circuits displayed in Fig. 5B and the obtained data are reported in Table 2.

Impedance spectra of the functionalised MWNT arrays and of the non-functionalised one show a large difference in the low frequency range. Indeed, non-functionalised array impedance spectra could be fitted with a classical Randles circuit (Fig. 5B) for which the Warburg contribution is taken as convective diffusion Warburg. This behaviour is in accordance with the electrode size of 150 μ m in diameter at which spherical diffusion takes place. In such a case, impedance modelling allows us to evaluate the interfacial capacitance (considered here as a pseudo-capacitance according to the surface roughness brought by the nanotube array) to be 0.2 μ F (1.13 mF cm^{−2}). Such a capacitance is rather low considering the developed surface associated with the nanotube array. Such behaviour is in accordance with the low wettability of the nanotube structure. Thereby, the nanotube array could only be considered as an “envelope” where only nanotube ends and walls placed at the periphery of the array are electrically active. In parallel, the obtained charge transfer

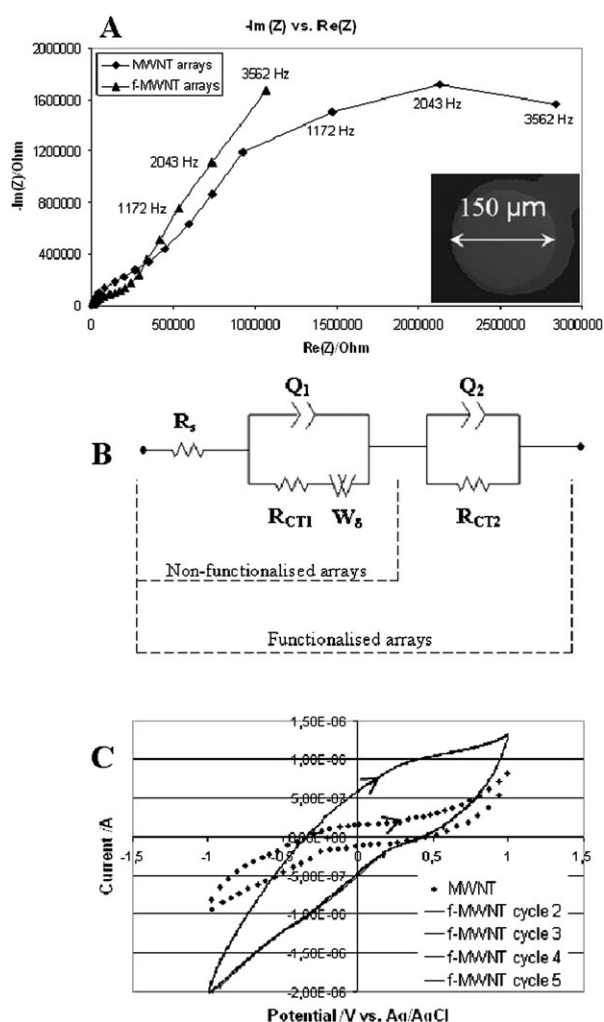


Fig. 5 (A) Impedance spectra of MWNT and *f*-MWNT arrays. Inset: SEM picture of the electrode surface with a diameter of 150 μm . (B) Electrical circuits used for fitting. R_s is the series resistance whereas R_{CT} represents charge transfer resistance. Q is a pseudo-capacitance and W_s is convective-diffusion Warburg impedance. (C) Cyclic voltammogram on the MWNT and *f*-MWNT arrays. The measurements were conducted in KCl (1 M) solution between -1 V and 1 V vs. Ag/AgCl reference at 100 mV s^{-1} .

Table 2 Parameters of the electrical circuit components used for the fitting of impedance spectra of functionalised and non-functionalised MWNT arrays

| | $R_s/\text{k}\Omega$ | $R_{CT1}/\text{k}\Omega$ | $Q_1/\mu\text{F}$ | $R_{CT2}/\text{k}\Omega$ | $Q_2/\mu\text{F}$ |
|--------------------|----------------------|--------------------------|-------------------|--------------------------|-------------------|
| Non-functionalised | 4.3 | 207 | 0.2 | — | — |
| Functionalised | 3.5 | 152 | 0.3 | 345 000 | 10.3 |

resistance is high (207 $\text{k}\Omega$). Such a high transfer resistance is in accordance with the electrochemical properties of MWNT for which only nanotube ends and defects are electroactive.¹⁸ In the case of PEG functionalised arrays, a second circuit composed of a pseudo-capacitance and a charge transfer resistance in parallel, could be added in series to the Randles circuitry (Fig. 5B). The Randles part of the circuit still represents a nanotube array envelope as already described. The obtained

electrical components are in accordance with the one previously obtained for the non-modified array. The circuit adjunction is related to low frequency compartment and could be associated to the “opening” of nanotube array nanoporosity owing to their enhanced wettability following functionalisation with PEG chains. Indeed, diffusion within such a constrained superstructure is slow. In such a way, the capacitance takes a high value of $10.3 \mu\text{F}$ (58.2 mF cm^{-1}) that highlights the large developed surface of the nanotube edifice. Concomitantly, the associated charge transfer resistance is very high (345 $\text{M}\Omega$) and is coherent with the electrochemical inertness of nanotube walls. Such behaviour was already reported by Wang *et al.* that modified a CNTs array by a lipid modified PEG chain.¹⁹ The authors obtained charge transfer resistances of modified and unmodified arrays of the same order whereas the capacitance values and enhancement recorded here show higher efficiency. Such differences may be related to the structure of the nanotube arrays.

Cyclic voltammeteries (Fig. 5C) in the same electrolytic solutions were performed to check the reliability of the impedance analysis and fitting. As expected, the voltamperogram associated with the PEG modified MWNT array shows an enhanced capacitive behaviour compared to the unmodified structure. The capacitance of MWNT, calculated from the cyclic voltammogram, is 8 mF cm^{-2} whereas it is increased to 31 mF cm^{-2} after functionalisation with **1**. These values are the same order of magnitude as those extracted from impedance spectra thus validating the reliability of the fitting.

Non-specific adsorption of streptavidin on the MWNT arrays

Previous studies have shown that proteins, such as streptavidin, can adsorb on the CNT surface through non-specific binding.²⁰ One of the main objectives of the MWNT array functionalisation by **1** is to prevent the non-specific adsorption of proteins on the surface. The adsorption of streptavidin on the MWNTs/Si and *f*-MWNTs/Si surface was first evaluated using Quantum dots covered with streptavidin (Qdots-streptavidin) in PBS ($1\times$, $\text{pH} = 7.4$) solution. The samples were characterised with a fluorescence microscope at an excitation wavelength of 546 nm, and the emission at 605 nm. Fig. 6 shows the fluorescence image of the MWNTs/Si (Fig. 6A) and *f*-MWNTs/Si (Fig. 6B) surfaces after the adsorption of streptavidin-Qdots. The red spots in the image correspond to the Qdot fluorescence, and denote the presence of streptavidin on the surface. We observed that a large amount of streptavidin is adsorbed on the MWNTs/Si surface, but there is almost no adsorption on the *f*-MWNTs/Si surface.

Another experiment consisted in the free streptavidin adsorption (without Qdots) on MWNTs/Si and *f*-MWNTs/Si, and analysis of the surface by XPS (Table S1, ESI†). The O% and N% of the MWNTs/Si surface increased strongly after incubation in the streptavidin solution, which is due to the presence of streptavidin on the surface. In the same experiment, the O% and N% of *f*-MWNTs/Si were unchanged. These results show that the functionalisation of MWNT arrays **1** is efficient in preventing the non-specific adsorption of proteins.

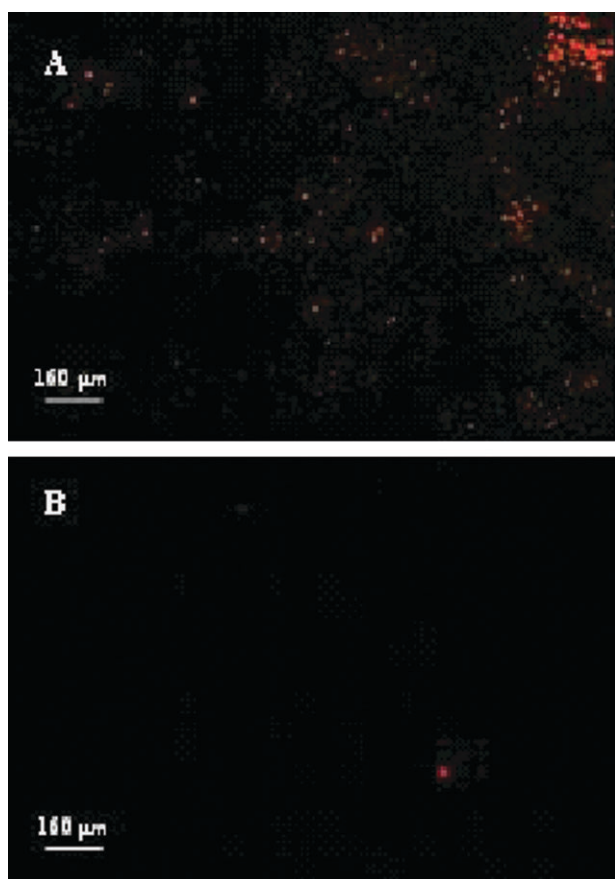


Fig. 6 Non-specific adsorption of Qdots-streptavidin on MWNTs/Si before (A) and after (B) functionalisation by **1**. The observation was performed with a fluorescence microscope (objective $\times 63$) with excitation wavelength of 546 nm and emission at 605 nm.

Conclusions

In summary, we have described in this paper a non-covalent functionalisation of CNTs by pyrene-PEG through π - π stacking. This functionalisation was first developed on MWNT powder, which shows a strong interaction between pyrene-PEG molecules and the MWNTs. The dialysis, used to remove free pyrene-PEG molecules in the suspension, did not lead to a diminution of MWNT-1 concentration. The percentage of coverage of the surface of the MWNT-1 by the pyrene moiety is about 20% after removal of all the free pyrene-PEG molecules in the suspension. Furthermore, the functionalisation is stable under extreme pH conditions, and also in high ionic strength solutions, which makes it possible to use this functionalisation in biological applications.

Secondly, we functionalised MWNT arrays with this method. This kind of functionalisation allowed retaining the MWNT conductivity (without creating further defects during the functionalisation) while increasing the electrode wettability and thus, the capacitance from 1.13 mF cm^{-2} to 58.2 mF cm^{-2} . In addition, the presence of pyrene-PEG

molecules is efficient in preventing the non-specific adsorption of streptavidin and Qdots-streptavidin.

Acknowledgements

This work was supported by the Agence Nationale pour la Recherche. We thank Dr Edward McRae (LCSM, UMR 7555 CNRS-UHP) for discussions. We thank Mr Claude Chabrol for his technical support. We also thank Mr Aurélien Fanton (LETI) and Mr Mathieu Dupoy (équipe commune biomerieux-LETI) for the XPS and fluorescence measurements, respectively. This work was carried out in the framework of the Nanobio program.

References

- 1 P. R. Kennedy, R. A. E. Bakay, M. M. Moore, K. Adams and J. Goldwaite, *IEEE Trans. Rehab. Eng.*, 2000, **8**, 198.
- 2 M. A. L. Nicolelis, D. Dimitrov, J. M. Carmena, R. Crist, G. Lehew, J. D. Krailik and S. P. Wise, *Proc. Natl. Acad. Sci. U. S. A.*, 2003, **100**, 11041.
- 3 (a) K. Wang, H. A. Fishman, H. Dai and J. S. Harris, *Nano Lett.*, 2006, **6**, 2043; (b) T. Gabay, M. Ben-David, I. Kalifa, R. Sorkin, Z. R. Abrams, E. Ben-Jacob and Y. Hanein, *Nanotechnology*, 2007, **18**, 035201–035206; (c) T. D. B. Nguyen-Vu, H. Chen, A. M. Cassell, R. Andrews, M. Meyya and J. Li, *Small*, 2006, **2**, 89–94; (d) E. W. Keefer, B. R. Botterman, M. I. Romero, A. F. Rossi and G. W. Gross, *Nat. Nanotechnol.*, 2008, **3**, 434–439.
- 4 Y. Lin, S. Taylor, H. Li, K. A. S. Fernando, L. Qu, W. Wang, L. Gu, B. Zhou and Y.-P. Sun, *J. Mater. Chem.*, 2004, **14**, 527–541.
- 5 B. Zhao, H. Hu, A. Yu, D. Perea and R. C. Haddon, *J. Am. Chem. Soc.*, 2005, **127**, 8197–8203.
- 6 J. Chattopadhyay, F. de Jesus Cortez, S. Chakraborty, N. K. H. Slater and W. E. Billups, *Chem. Mater.*, 2006, **18**, 5864–5868.
- 7 J.-C. Charlier, *Acc. Chem. Res.*, 2002, **35**, 1063–1069.
- 8 M. Shim, N. W. S. Kam, R. J. Chen, Y. Li and H. Dai, *Nano Lett.*, 2002, **2**, 285–288.
- 9 H. Dai, N. W. S. Kam, P. A. Wender and Z. Liu, United States Patent 20060275371.
- 10 N. Nakayama-Ratchford, S. Bangsaruntip, X. Sun, K. Welsher and H. Dai, *J. Am. Chem. Soc.*, 2007, **129**, 2448–2449.
- 11 A. Peigney, Ch. Laurent, E. Flahaut, R. R. Bacsá and A. Rousset, *Carbon*, 2001, **39**, 507–514.
- 12 R. J. Chen, Y. Zhang, D. Wang and H. Dai, *J. Am. Chem. Soc.*, 2001, **123**, 3838–3839.
- 13 (a) N. Nakashima, Y. Tomonari and H. Murakami, *Chem. Lett.*, 2002, 638–639; (b) D. M. Guldi, G. M. A. Rahman, N. Jux, N. Tagmatarchis and M. Prato, *Angew. Chem., Int. Ed.*, 2004, **43**, 5526–5530; (c) D. M. Guldi, G. M. A. Rahman, N. Jux, D. Balbinot, N. Tagmatarchis and M. Prato, *Chem. Commun.*, 2005, 2038–2040.
- 14 K. A. S. Fernando, Y. Lin, W. Wang, S. Kumar, B. Zhou, S.-Y. Xie, L. T. Cureton and Y. P. Sun, *J. Am. Chem. Soc.*, 2004, **126**, 10234–10235.
- 15 D. M. Guldi, G. M. A. Rahman, N. Jux, D. Balbinot, U. Hartnagel, N. Tagmatarchis and M. Prato, *J. Am. Chem. Soc.*, 2005, **127**, 9830–9838.
- 16 N. Nakashima, *Sci. Technol. Adv. Mater.*, 2006, **7**, 609–616.
- 17 J. Liu, M. Rodriguez i Zubiri, B. Vigolo, M. Dossot, Y. Fort, J.-J. Ehrhardt and E. McRae, *Carbon*, 2007, **45**, 885–891.
- 18 J. Yan, H. Zhou, P. Yu, L. Su and L. Mao, *Adv. Mater. (Weinheim, Ger.)*, 2008, **20**, 2899–2906.
- 19 K. Wang, H. A. Fishman, H. Dai and J. S. Harris, *Nano Lett.*, 2006, **6**, 2043–2048.
- 20 F. Balavoine, P. Schultz, C. Richard, V. Mallouh, T. W. Ebbesen and C. Mioskowski, *Angew. Chem., Int. Ed.*, 1999, **38**, 1912–1915.